Proceedings of: JRC2002
The 2002 ASME/IEEE Joint Rail Conference
April 23-25, 2002, Washington D.C.

VEHICLE POSTMORTEM AND DATA ANALYSIS OF A PASSENGER RAIL CAR COLLISION TEST

Robert A. MacNeill and Steven W. Kirkpatrick
Applied Research Associates, Inc.
2672 Bayshore Parkway, Suite 1035
Mountain View, CA 94043

ABSTRACT

There is an ongoing research program in the United States to investigate and improve rail equipment crashworthiness. As part of this effort, a series of full-scale rail vehicle crash tests are being performed to investigate the crash response of existing and future rail vehicle designs. The first full-scale test, an impact of a single passenger coach car into a fixed wall, was conducted at the Transportation Technology Center (TTC) in Pueblo, Colorado on November 16, 1999. The test vehicle used was a Pioneer passenger coach car. The test condition was a 35 mph impact into a fixed rigid concrete wall.

Collision response data was collected in the test using accelerometers, strain gauges, string potentiometers, and high-speed photography. This paper describes the postmortem documentation and data analysis process. The objective is to develop an understanding of the vehicle collision response and to obtain a consistent correlation of the various sources to data. Specific documentation and data analysis techniques used for the study are described along with key results.

INTRODUCTION

This paper describes the vehicle postmortem and data reduction for the Pioneer Single car test performed at TTC in November of 1999 [1-3]. The vehicle pretest and posttest is shown in Figure 1. The overall program objectives were twofold: first, a vehicle postmortem and data reduction was to be performed and, second, a detailed finite element model predicting the crush behavior and vehicle gross motions was to be generated. The postmortem and data analysis not only supplied a deep understanding of the crash events but provides a means for validating the numerical model. A companion paper describing the vehicle crash modeling is Reference 4.

Given the volume of the collected data generated by the postmortem and data reduction process, only a subset is presented here. Of primary focus are the high-speed film, string potentiometer, and longitudinal accelerometer data. Vertical and lateral accelerometer data is briefly described as well. Strain gauge data was analyzed but is not addressed in this paper. Additional analysis of the data is contained in Reference 5.

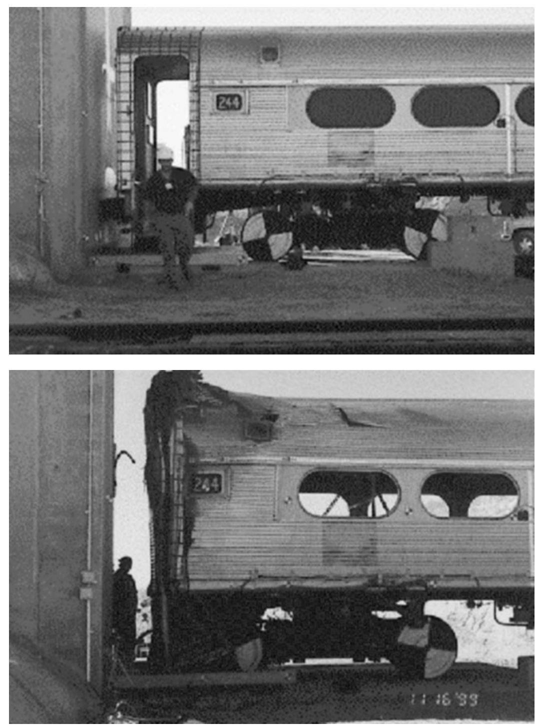

Figure 1. Photographs of the Single Coach Car Crash Test

The overall vehicle crash response featured a crush behavior consisting of an approximate 7-g crash deceleration and approximately 66 inches of peak crush (54 inches after relaxation). Inspection of the vehicle showed that the draft sill was the dominant structural component and was expected to have dissipated a significant fraction of the collision energy.

The vertical and lateral motions of the vehicle were much smaller than the longitudinal motions. The vertical motion of the car body consisted of an upward lifting of the forward car body with a maximum displacement of approximately 5.5 inches. The vertical car body motion consisted of both an extension of the secondary suspension to its limit of approximately 2.5 inches and a subsequent lift of the front truck off the rails of approximately 3 inches. The analysis of the lateral accelerometer measurements indicated a rotation with the front end of the occupant compartment displaced approximately 9 inches to the left side and the rear of the car displaced approximately 2 inches to the right.

EQUIPMENT POSTMORTEM

The objective of the equipment postmortem was to document the deformation modes of the principal structural members. The test vehicle, shown in Figure 2, was a Budd Pioneer passenger coach car. The Pioneer cars, intended to be a low-cost, lightweight passenger car, were designed in the late 1950s and built through the 1960s.

Figure 2. Pretest Budd Pioneer Passenger Coach Car

The car body structures of the vehicle prior to the test were intact with the exception of the original seats and some auxiliary equipment removed from the vehicle. A few prototype seats and crash dummies were added to the vehicle interior to study occupant protection strategies [3]. In order to account for the weight difference of the removed equipment, approximately 10,000 lbs of concrete was added to the test vehicle as ballast to increase the test weight.

As part of the equipment postmortem, a large number of photographs and sketches were taken of the vehicle. These included documentation of the damaged structural components and the undamaged components on the vehicle B-end (the vehicle was impacted on the A-end). The photographs and sketches of the undamaged components were to document the geometry of the vehicle structures not included in the available car body blueprints.

The impact speed of the test vehicle was measured at 35.1 mph. The overall crash deformation of the car body is shown in Figure 3. The observed crash response features a complete collapse of the car end structures in the vestibule and deformations that extend into the occupant compartment behind the vestibule bulkhead wall. The overall reduction in the car body length from the crush deformations measured after the test was approximately 54 inches (reduction in length between the A-end body bolster and buffer beam). The upper portion of the superstructure in the vestibule had nearly completely failed as shown in Figure 3. As a result, the car body end wall was primarily attached to the remainder of the car body by the deformed under frame components.

Figure 3. Front and Right Side Car Body Crash Deformations

An inspection of the vehicle interior at the impact end found that virtually all of the survivable space within the vestibule was eliminated. In addition, the floor immediately aft of the vestibule bulkhead wall was buckled upward and the bulkhead intruded into the first row of seats. The upper plate section of the draft sill was torn away from the draft sill and pushed upward through the floor in this section.

The draft sill is the largest structural member in the car so its collapse mode is significant in the vehicle crash response. The draft sill inspection showed complex collapse mechanisms that were different on either side of the vehicle. Figure 4 shows a photograph of the right side draft sill response.

On this side, the forward draft sill was pushed back and slightly downward with little plastic deformation. The collapse of the draft sill right side occurred in a region immediately aft of the bulkhead wall. This location would see very high loading in the early phase of the crash response because the draft gear impact was reacted by an internal plate in the draft sill below the bulkhead (the buff stop). A corresponding sketch of the right side draft sill collapse mode is shown in Figure 5. The sketch indicates the overall reduction in draft sill length measured 54 inches.

Figure 4. The Draft Sill Right Side Collapse Mode

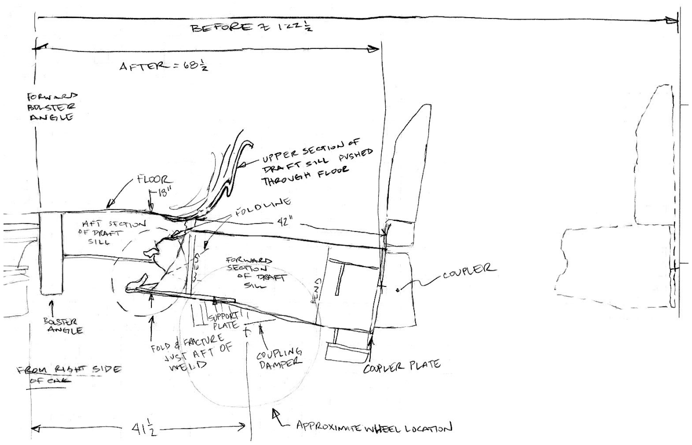

Figure 5. Sketch of the Draft Sill Right Side Collapse Mode

A photograph of the left side draft sill response is shown in Figure 6. On this side, the draft sill was buckled outward and formed several plastic hinges. The collapse of the left side was distributed over a significant length of the sill including the forward section that was relatively undeformed on the right side. The mechanisms that contributed to this forward sill collapse cannot be fully determined from the inspection. However, contributing factors could be an early time fracture of the buff stop weld on the left side and/or a failure of the pilot connection to the draft sill on the left side. The pilot structures were attached below the draft sill in a configuration that would help to reinforce the forward draft sill.

A sketch of the overall draft sill collapse mode is shown in Figure 7. The sketch illustrates the draft sill collapse modes. The large difference in response on the two sides of the vehicle is can be seen in the figure.

A brief inspection of the forward draft sill collapse modes in the subsequent two car collision test showed two different modes of collapse on either side of the draft sill than observed here. This variability in the collapse mechanism results from a vehicle designed to meet strength requirements rather than crash energy management designs where a controlled collapse mechanism is introduced. In the strength design approach, the most efficient design has a relatively uniform strength throughout the structure. As a result, the specifics of the collapse modes can be changed by small differences in the local geometry or by variability in the loading conditions.

Figure 6. The Draft Sill Left Side Collapse Mode

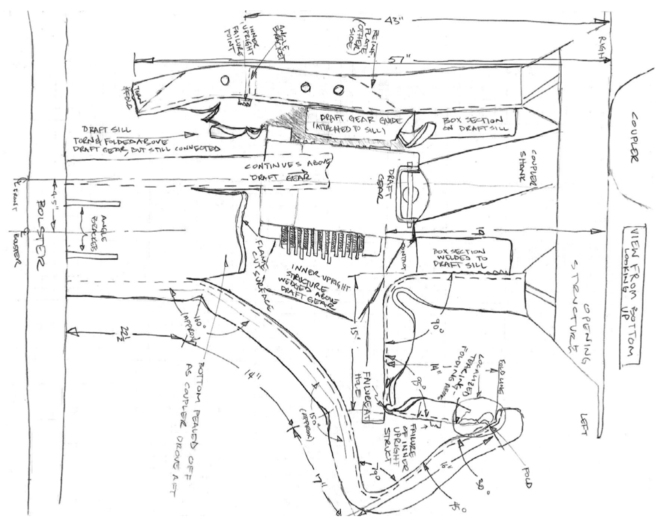

Figure 7. Sketch of the Overall Draft Sill Collapse Mode – View from Bottom

The collapse of the car body structures aft of the bulkhead wall was significantly less than in the forward vestibule crush zone. The side sill was buckled in a couple of positions near the impact end, however, the overall damage and change in length was relatively small. The side sill damage on the left side of the vehicle was even less than that seen on the right side.

DATA POSTPROCESSING

An important contribution to understanding the overall crash response of the vehicle is to analyze all of the quantitative data collected. This includes the measurements from the accelerometers, string potentiometers, strain gauges, and high-speed film. The objective is to evaluate all of the data to obtain a clear and consistent interpretation of the measured collision response both in the crush zone and the remaining occupant compartment and car structures. An additional objective is to reduce the data to a form for easy comparison and validation of collision models.

The measurements and associated data analyses are presented below. Because of the volume of the data analyzed, only a sampling of the high-speed film, string potentiometer, and accelerometer data are presented here. We begin with the analysis of the high-speed film data because it provides the most straightforward measurements of both vehicle crush and gross motions. Subsequent analysis of the data collected can then use the photographic data as a reference for consistency.

HIGH-SPEED FILM

The high-speed photographic data was previously analyzed to obtain the quantitative vertical and longitudinal motions of the front end of the car body [2]. In that analysis, the film was projected frame-by-frame onto a digitizer pad and the locations of three vehicle-mounted and three ground-based reference targets were recorded. The displacements were calculated as the relative motion between the average of the three targets on the vehicle and the average of the three on the ground. The displacement reference distance was obtained between the two extreme ground based targets that were spaced 88 inches apart.

The longitudinal displacements obtained from the east (left side) and west (right side) high-speed cameras are shown in Figure 8. The film data indicates a maximum crush distance of 65.8 inches on the left side and 67.2 inches on the right side of the vehicle at approximately 0.23 seconds.

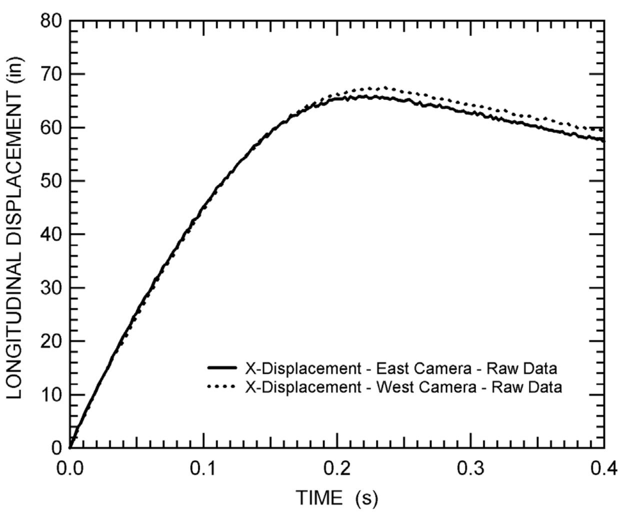

Figure 8. Longitudinal Displacement from High-Speed Film

The displacements from the high-speed photographic data were differentiated on a frame-by-frame basis to obtain velocities. The nominal film speed was 500 fps and the exact time step per frame was obtained from 100 Hz timing marks on the film. The longitudinal velocities obtained from the east and west cameras are shown in Figure 9. This velocity data was smoothed using a low-pass phaseless 4th-order Butterworth filter with a cutoff frequency of 23 Hz.

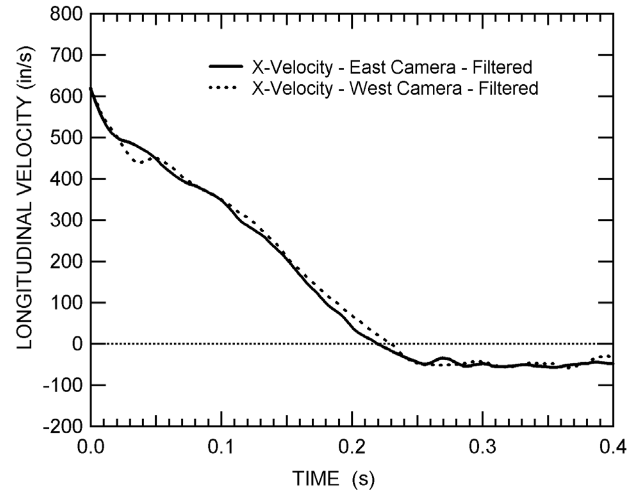

Figure 9. Longitudinal Velocity from High-Speed Film

An examination of the longitudinal velocity data shows an approximately linear deceleration from the initial velocity of 618 in/s (35 mph) to a final rebound velocity of approximately -50 in/s (3 mph). The duration of the crash response was approximately 0.25 seconds beyond which the vehicle has rebounded from the wall.

If we again differentiate the filtered longitudinal velocity curves, we can obtain the longitudinal crash deceleration pulse from the high-speed film as shown in Figure 10. The vehicle crash deceleration pulse shows an initial spike as the vehicle hits the wall. The subsequent crash pulse duration is approximately 0.25 seconds and has an average amplitude of about 7-g.

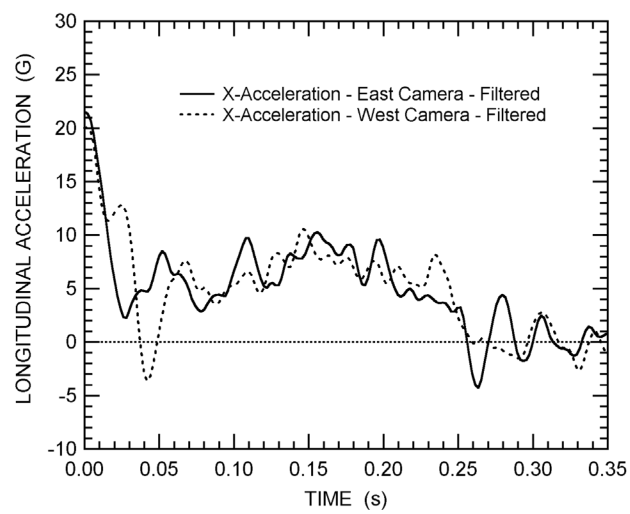

Figure 10. Longitudinal Acceleration from High-Speed Film

The vertical displacements obtained from the high-speed cameras are shown in Figure 11. This graph shows a frame-by-frame variation on the order of ±0.5 inches giving an estimate of the maximum resolution error on the film displacement measurement. The film data indicates a maximum vertical lift of 4.2 inches on the left side and 5.3 inches on the right side of the vehicle at a time of between 0.25 and 0.40 seconds. The majority of the vertical lifting motion occurs between 0.1 and 0.25 seconds.

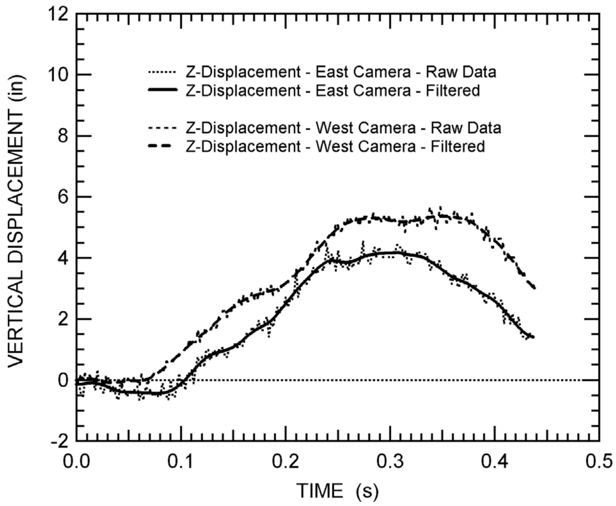

Figure 11. Vertical Displacement from High-Speed Film

The filtered vertical velocities obtained from differentiating the high-speed camera displacement data are shown in Figure 12. The figure shows that the vertical velocity magnitudes vary in the range between approximately 10 to 40 in/s during the crash response from approximately 0.1 to 0.25 seconds. The subsequent velocity history shows that the vertical velocities dropped at an average rate equal to a 1-g deceleration. This behavior is consistent with a gravitational free fall of the front end of the vehicle after the impact face rebounded from the wall (0.25-0.42 seconds). Therefore, the vertical velocity histories obtained from analysis of the high-speed film are consistent with the observed crash response.

STRING POTENTIOMETER DATA

Four string potentiometers were included in the single car impact test with the objective of measuring the relative vertical displacements between the bolster and the trucks (secondary suspension motion). The string-potentiometers were used to measure the relative vertical displacement between the vehicle bolster and the trucks on the right and left sides of the vehicle.

Because of instrumentation problems, no data was recorded for the B-end right side potentiometer. The A-end potentiometers measured a positive displacement (extension) that varied between 0.6-3.6 inches after the initial impact response. The B-end potentiometer measured displacements varied between 0.8 inches in extension to 1.5 inches in compression. The late time B-end measurement is primarily compressive but the absence of the right side B-end measurement makes it impossible to determine if this is a result of compression across the suspension or from roll of the car body relative to the trucks. The late time magnitudes of the A-end measurements indicate car body roll toward the left side relative to the truck position.

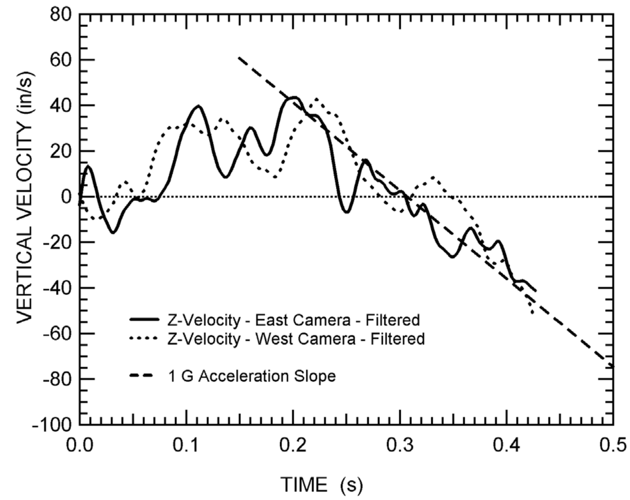

Figure 12. Filtered Vertical Velocity from High-Speed Film

An analysis of the A-end string potentiometer data is shown in Figure 13. Included in the figure is an average of the measurements from the right and left sides and the vertical car body displacements as measured from the west side high-speed camera. The comparison shows that the early time vertical motions of the car body, up to a time of approximately 0.16 seconds, is facilitated by extension of the secondary suspension (the vertical car body motion is equal to the string potentiometer extension).

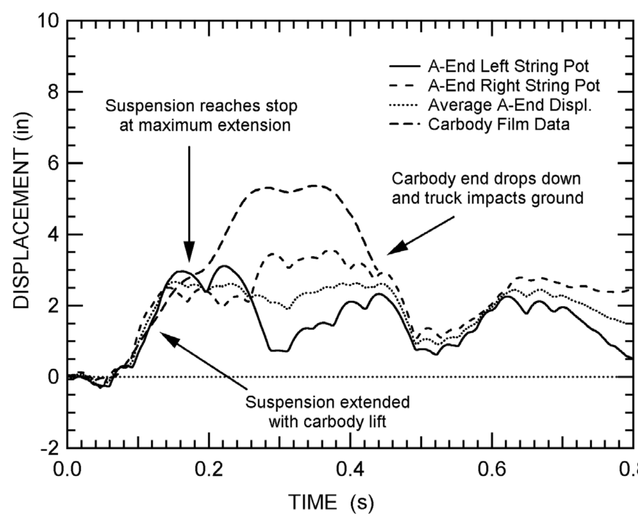

Figure 13. Suspension and Vertical Car Body Motion Data Comparison

The measured potentiometer data shows that the secondary suspension reaches its extension limit between 0.16 to 0.46

seconds. This is indicated by the relatively uniform extension of the average potentiometer displacement at approximately 2.5 inches. The difference between the extensometer displacement and the car body displacement during this time interval is equal to the vertical lift of the trucks relative to the track. Thus the measurements indicate a vertical lift of the front truck of approximately 3 inches between 0.26 and 0.38 seconds.

The late time vertical motions show that the trucks would fall back to the rail/ground at a time between 0.42 and 0.48 seconds. At this time the car body vertical lift was again approximately equal to the potentiometer extension. The subsequent potentiometer data shows some compression of the suspension between the times of 0.45 and 0.5 seconds at a rate approximately equal to the slope at which the car body was dropping. The potentiometer extension remains positive for all of the subsequent motions due to the deformation of the draft sill and other structures in the crush zone that interfere with the clearances between the car body and truck. Some of these deformed car body structures were cut away before the damaged vehicle could be moved from the crash site.

ACCELEROMETER DATA

The acceleration data was analyzed in detail to determine effects associated with measurement uncertainty, to obtain the best possible estimates of the vehicle motions from the acceleration integration, and to determine the operational mode shape characteristics of the car structure.

Accelerometers were used to measure the vehicle response in the longitudinal, vertical, and lateral directions at various points on the vehicle under frame. The distribution of accelerometers on the test vehicle is shown Figure 14. The majority of the accelerometer data was successfully recorded, however, some acceleration measurements were lost due to instrumentation failures. The 100-g lateral accelerometers at both the right and left position 1 locations saturated from larger than expected magnitudes of acceleration. The vertical accelerometers at the right side positions 1 and 2 also saturated. In addition, the cable failed on the center position 1 accelerometer early in the crash response, and the accelerator mounting integrity for the right front accelerometer location was compromised because of a loose mounting plate producing a resonance in the measured accelerations.

Beyond the failures of accelerometer channels, the two significant sources of uncertainty identified in the acceleration measurements are (1) the resolution of the recording system, and (2) the potential for cross axis contamination. The accelerometer data was recorded using a 12-bit digital recording system and a full-scale potential range of ±2.5 Volts, giving a resolution of 1.2 mV. The accelerometer sensitivity for a 200-g accelerometer is 10 mV/g. The resulting resolution of the data acquisition is 0.12-g (47 in/s^2). The presence of this baseline resolution error (constant DC-offset), when double integrated to compute displacement over the 1.4 sec. duration of the impact event record, produces a 46-inch maximum displacement error.

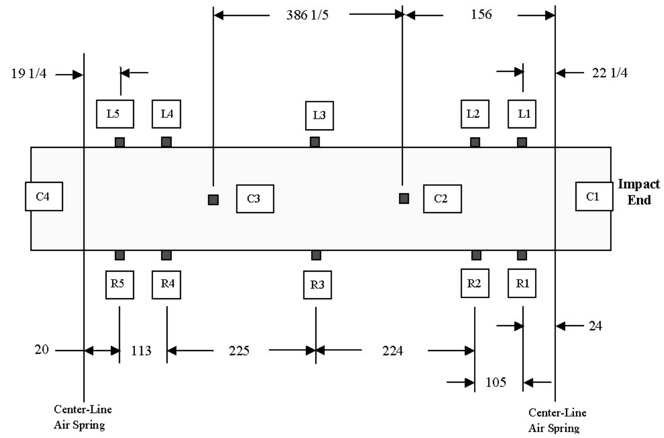

Figure 14. Measured Test Vehicle Accelerometer Positions

In addition to bias error affecting all measurements, cross-axis contamination of lateral and vertical acceleration measurements resulting from the larger amplitude longitudinal accelerations must be considered. A shaker test was performed and measured a cross-axis sensitivity of 2% on average.

The longitudinal acceleration pulse of the impact is sufficient to produce a change in longitudinal velocity of 37 mph (670 in/s) in approximately 0.25 second. Assuming a 2% cross-axis contamination error, this large longitudinal signal results in a corresponding cross-axis error in the measurement of lateral and vertical velocities of approximately 13 in/s. When integrating over the remainder of the record to obtain displacements, this error produces a corresponding error in lateral and vertical displacements of approximately 17 inches.

Longitudinal Accelerometer Data

The longitudinal accelerations measured at positions along the right side sill are shown in Figure 15. These records have been filtered using an SAE 60 Hz filter and are typical of the measurements on the vehicle under frame. Comparing the records shows differences in the details of the pulse shapes and peak magnitudes. However, on average, the records have a similar character with an early time peak acceleration followed by a rapid drop to low accelerations and a subsequent average deceleration magnitude of approximately 7-g.

A corresponding average deceleration pulse for the longitudinal accelerometer records is given in Figure 16. This average acceleration record clearly indicates the form of the characteristic longitudinal crash pulse shape. As a consistency check, we can compare the longitudinal accelerations obtained from analysis of the high-speed film with the accelerometer data. The average of the east and west side high-speed film acceleration, shown previously in Figure 10, is compared to the average accelerometer longitudinal crash pulse in Figure 16. The comparison shows good agreement in both the shape and magnitude of the longitudinal crash pulse.

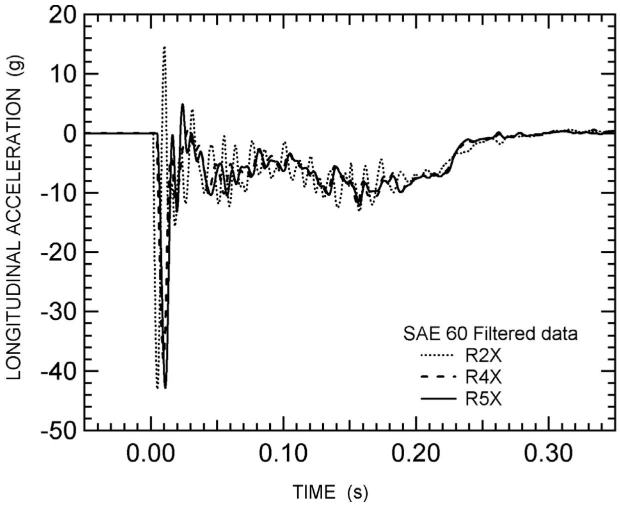

Figure 15. Right Side Sill Longitudinal Accelerations

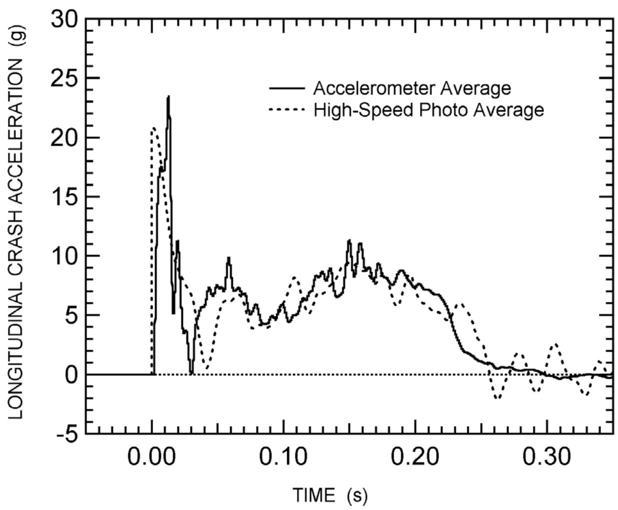

Figure 16. Accelerometer and High-Speed Film Comparison

Cross contamination is not expected to produce significant error in these longitudinal accelerations because the average acceleration amplitudes for vertical and lateral directions are an order of magnitude smaller. However, the resolution of the recording system is an issue. To account for the error, a correction coefficient was added to the acceleration magnitudes that results in a rebound velocity of 50 in/sec.

The integrated longitudinal velocities and displacements obtained from the corrected acceleration records are shown in Figure 17 and Figure 18, respectively. After correction, the peak displacements range from 64 to 68 inches. These agree well with the maximum longitudinal displacement obtained from the film analysis of approximately 66 to 67 inches.

Vertical and Lateral Accelerometer Data

The vertical and lateral accelerometer data will have errors introduced by both the data recording resolution bias error and cross axis contamination. The difficulty is that the magnitudes of the vertical and lateral displacements being measured were smaller than the overall magnitudes of the errors in the data. The displacement histories obtained by double integration of the raw vertical accelerations at the various car body positions are diverging with displacements in the range of –70 to 32 inches at the end of the 1.5 second record. Therefore, the raw data cannot be used to estimate the vertical and lateral behavior without a significant data reduction analysis to eliminate the errors in the collected data.

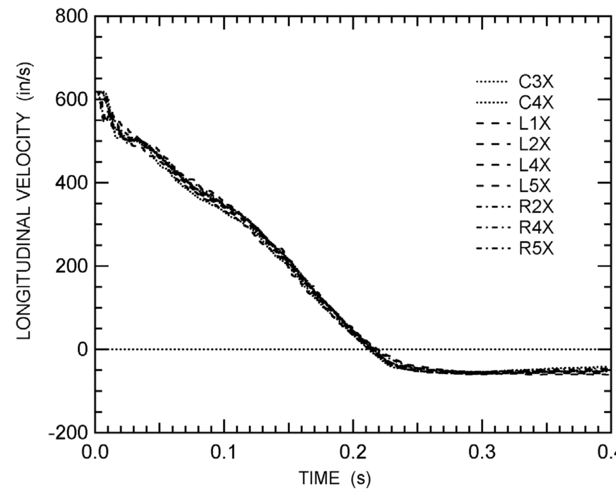

Figure 17. Corrected Integrated Velocities

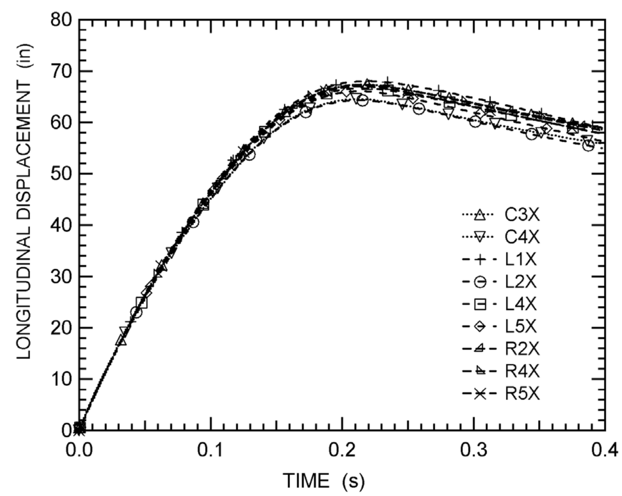

Figure 18. Corrected Integrated Displacements

The physical information used to correct the data is that at late times the vertical and lateral velocities of the car body will be zero on average (the vehicle comes to rest). For the 1.5 second duration recorded here, the vertical and lateral accelerations should, therefore, be oscillating about zero for approximately the last 0.8 seconds. Corrections were applied to resolve cross-axis contamination and baseline resolution errors in the data. The magnitudes of these corrections are selected such that both the magnitude and slope of the late time lateral and vertical velocities are effectively zeroed. A cross-axis contamination correction will produce a shift in the magnitude of the late time velocity, while a baseline resolution error correction will change the slope of the late time velocity. The resulting corrected velocity histories were then integrated to obtain lateral and vertical displacements.

A correction of the vertical and lateral accelerometer data was performed. The displacements obtained by double integrating the left side corrected acceleration histories are compared to the vertical displacements obtained from the high-speed photography in Figure 19. The vertical displacements obtained from the L1Z accelerometer agree well with the high-speed photography data. The displacement histories indicate a vertical car body response dominated primarily by rigid body displacements and rotations.

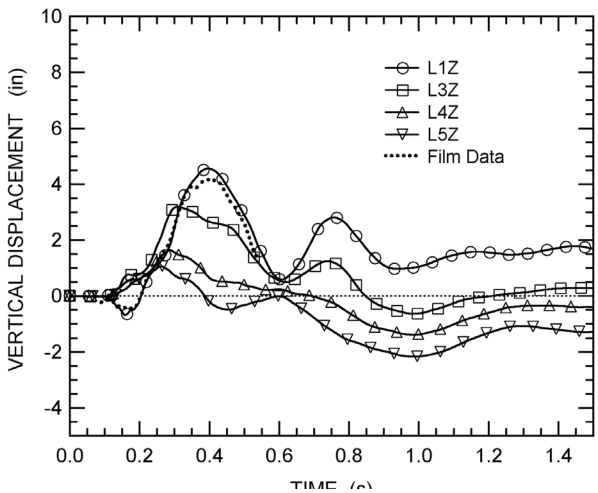

Figure 19. Vertical Displacements Obtained from Analysis of Accelerometer Data

The data correction procedure performed for the lateral accelerations was identical to that used for the vertical accelerations. The displacements obtained by double integration of both the left and right side corrected lateral acceleration histories are shown Figure 20. The first observation about the displacements is the good agreement between the left and right side displacements. Agreement between the right and left sides is expected because of the small lateral deformations across the car body under frame between the corresponding left and right side accelerometer positions. This agreement between independent corrections of the left and right side data provides a level of confidence in the data reduction process.

CONCLUSIONS

Performing the vehicle postmortem and data analysis provided a better understanding of the collapse mechanisms, damage progression, and crash dynamics in the single car collision test. Also, the reduced data provides a quantitative means for comparison with crash analyses such as the FEA model described in Reference 4. The knowledge gained by performing the postmortem and high-speed film analysis proved important in accurately reducing the accelerometer data. The good agreement when comparing displacements and accelerations from the independent high-speed film and accelerometer data gives added confidence in the results.

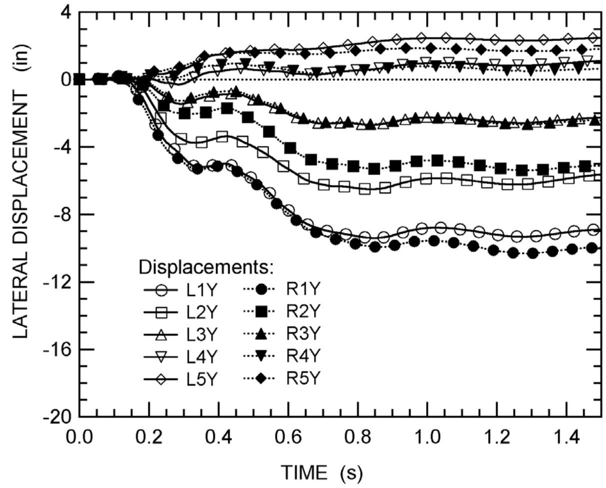

Figure 20. Lateral Displacements Obtained from Analysis of Accelerometer Data

ACKNOWLEDGEMENTS

The work described in this paper was performed under contract to the Volpe Center, as part of the Equipment Safety Research Program sponsored by the Federal Railroad Administration (FRA). The contract was initiated and monitored by David Tyrell and Kristine Severson, Senior Engineers, Structures and Dynamics Division, Volpe Center. Tom Tsai, Program Manager, Equipment and Operating Practices Research Division, FRA, manages the passenger rail equipment crashworthiness research.

REFERENCES

1. Tyrell, D., Severson, K., Perlman, A.B., “Single Passenger Rail Car Impact Test Volume I: Overview and Selected Results,” US DOT, DOT/FRA/ORD-00/02.1, Mar. 2000.
2. VanIngen-Dunn, C., “Single Passenger Rail Car Impact Test Volume II: Summary of Occupant Protection Program,” US DOT, DOT/FRA/ORD-00/02.2, Mar. 2000.
3. Brickle, B., “Single Passenger Rail Car Impact Test Volume III: Test Procedures, Instrumentation, and Data,” US DOT, DOT/FRA/ORD-00/02.2, May 2000.
4. Kirkpatrick, S.W., & MacNeill, R.A., “Development of a Computer Model for Prediction of Collision Response of a Railroad Passenger Car,” Proc. JRC2002, The 2002 ASME/IEEE Joint Rail Conference, Washington D.C., Apr. 23-25, 2002.
5. Kirkpatrick, S.W., MacNeill, R.A., & Shroeder, M., “Development of Computer Model for Prediction of Car Crush and Gross Motion of a Railroad Passenger Car Under Collision Conditions,” Draft Final Report, Volpe National Transportation Systems Center, 2001.